



ÉCOLE POLYTECHNIQUE FÉDÉRALE DE LAUSANNE

Project 2

Final Project

CS 432 - COMPUTATIONAL MOTOR CONTROL

Students: Nina Lahellec (327695), Marine Moutarlier (310703),
Marianne Civit Ardevol (325056)

July 20, 2024

Contents

Questions	2
3. Implement the equations for the firing rate controller	2
4. Explore the dependency on the descending input drive I	5
5. Test the firing rate controller swimming behavior and turning	7
5.1. Swimming behavior of neuromechanical zebrafish, individual simulation	7
5.2. Measuring turning performance	7
5.3. CPGs and MCs activities depending on I_{diff}	9
6. Implement the feedback equations and test different feedback weights	11
6.1. Role of sensory feedback for fixed parameters	11
6.2. Influence of the feedback weight on the frequency, wave frequency and forward speed	12
6.3. Conditions under which feedback weight is beneficial	14
7. Explore the dependency on the descending input I and feedback weight g_{ss}	15
7.1. Repeat analysis of question 5 for different values of g_{ss}	15
7.2. How does the frequency and wavefrequency change with the added feedback?	
Does the ranges of inputs I leading to stable oscillation change? What about	
the performance (i.e. forward speed) for these ranges of I , does it change? . . .	16
8. Explore the effect of noise with/o feedback	20
9. Open question	23

Warning: code running instructions

- In order to run the `plot_results.py` file, please use this format to indicate for which exercise the plots are desired:

```
python plot_results.py exercise_nb
```

- As for question 5 and 6, since there are different plots depending on if there is a simple or multiple simulations, the files `exercise5.py` and `exercise6.py` have to be run directly in order to get the plots. Comment/De-comment to get simple or multiple simulations, with the respective plots.
- Also for clarity reasons, we separated the `firing_rate_controller.py` into
 1. `firing_rate_controller_open_loop.py`
 2. `firing_rate_controller_close_loop.py`.
- Also to run the `exercise7.py`, please put the corresponding index for the `w_stretch` to correctly load the corresponding controller. See line 19 in `exercise7.py`

```
def main(ind=0, w_stretch=15): # run for w_stretch = 0, 4, 8, 12, 15 (ind = 0, 1, 2, 3, 4)
```

- Same, please load the correct path that you want to read while plotting the results from `plot_results.py` (see line 225)

```
if exercise_nb == 7:  
    controller = load_object("logs/exercise{}/w_stretch0/controller{}".format(exercise_nb,  
        ↪ controller_nb)) # replace with w_stretch0 or w_stretch1 or w_stretch2 or w_stretch3 or  
        ↪ w_stretch4
```

Questions

3. Implement the equations for the firing rate controller

Implement the open loop firing rate controller in ?? without the feedback terms (omit the terms $g_{ss}W_{ss} \cdot \underline{s}_R$ and the sensory feedback neuron equations for \dot{s}_L and \dot{s}_R). Run the network for fixed default parameters and plot the CPG and MC activities. Demonstrate that the network with default parameters supports an oscillatory traveling wave of activity propagating from the head to the tail and use the metrics to quantify frequency, amplitude, wavefrequency, ptcc.

3. Answer

When running the network in open loop for 5 seconds, the obtained plots for muscle activities and CPG activities are the following:

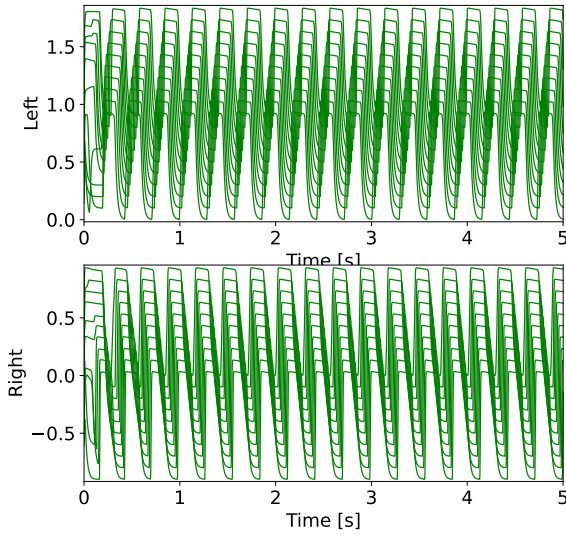


Figure 1: Left-right plot of the muscle activities for default values of the parameters

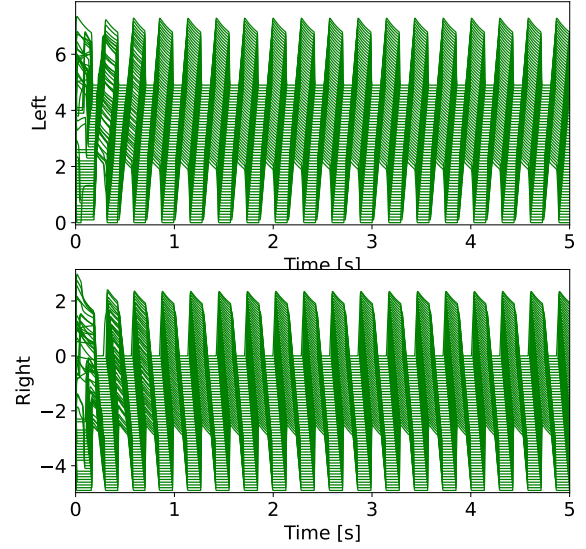


Figure 2: Left-right plot of the CPG neuron activities for default values of the parameters

It can be seen that there is a travelling wave in both activities. Indeed, the plots show that the oscillations don't occur always at the same time, they are offset by a constant for each muscle and CPG that is active.

Furthermore, the plots show that the travelling wave is from head to tail. Indeed, the right muscle activity shows that the muscles closer to the head (at the top) are active before those at the tail (lower part of the y-axis). This indicates that the muscles activate one after the other, from head to tail. Looking at the left muscle activities, the signal is symmetric and here the bottom section of the y-axis represents the tail of the fish and the top section of the y-axis represents the head.

The metrics obtained in this implementation are the following:

Metric	Value
Frequency	3.4836
IPLS	0.1819
Wave Frequency	0.6337
PTCC	1.8563
Amp	1.8378

Table 1: Computed Metrics for default parameters

Since the values for the neuron timescale and adaptation timescale are $\tau = 0.002$ and $\tau_a = 0.3$, the frequency can be derived with

$$f = \frac{1}{\tau + \tau_a} = \frac{1}{0.002 + 0.3} \approx 3.311 Hz$$

Therefore, the computed metric for the frequency of $3.48 Hz$ is accurate and seems to follow the model correctly.

Furthermore, the value computed for the ptcc metric is close to zero which indicates the fish is swimming in its stable state.

Concerning the wavefrequency, it is expected to observe a non-zero and positive wavefrequency. This would indicate that there is a travelling wave from head to tail in the CPGs. As explained above, the figures 1 and 2 do indicate that there is indeed a forward travelling wave and confirms the obtained

non-zero, positive wavefrequency metric value of 0.6337.

This wavefrequency comes from the asymmetry in the designed model. The figure below from the project description illustrates this phenomena :

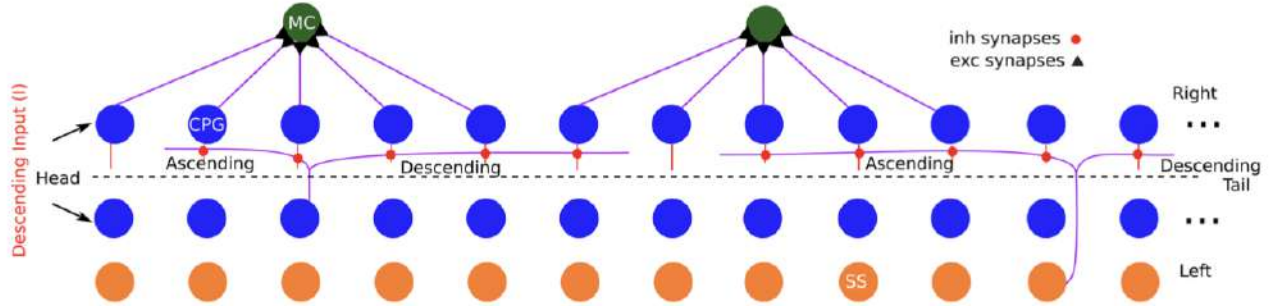


Figure 3: Figure 3 of the project description, showing the sketch connectivity of the neural model

Indeed, the CPG neurons inhibit their neighbouring neurons in an asymmetric manner. It can be observed that a single CPG neuron will inhibit only 2 of its ascending CPG neighbours and 3 of its descending CPG neighbours. This creates the forward travelling wave and the positive wavefrequency.

Contrary to project 1, the amplitude metric computes the limb amplitudes. This is why the computed metric does not correspond to the amplitudes in muscle activities plot in figure 1. Since here we are in open loop, we don't analysing the amplitude metric is not very informative.

4. Explore the dependency on the descending input drive I

The descending input parameter I represents the excitation to the CPG network from higher brain centers. Vary $I \in [0, 30]$ in the system and test the ranges of descending inputs that support oscillations (you can use the $ptcc$ metric to measure the stability of the oscillations). How does the frequency and wavefrequency change within the range of I that support the oscillations?

4. Answer

In order to find the values for I that support oscillations we first swept through all of the values of $I \in [0, 30]$ and looked for which of these the values of $ptcc$ were above 0.5 ($ptcc > 0.5$ indicates stable oscillations). Through this procedure, it has been found that for I in the range of $[4, 22]$, the oscillations are stable. The plot below illustrates this:

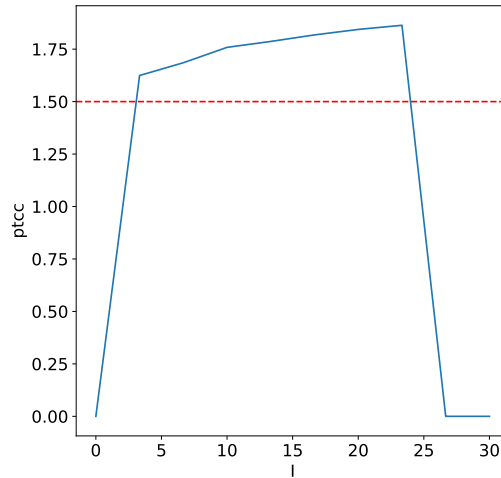


Figure 4: Evolution of the $ptcc$ value with respect to the descending input parameter I vary

With these values of I , plots were generated showing how the frequency and wavefrequency vary depending on $I \in [0, 30]$:

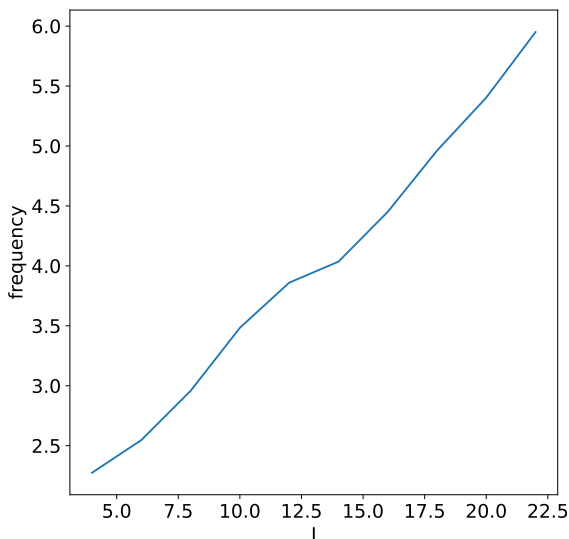


Figure 5: Evolution of the frequency with respect to the descending input parameter I

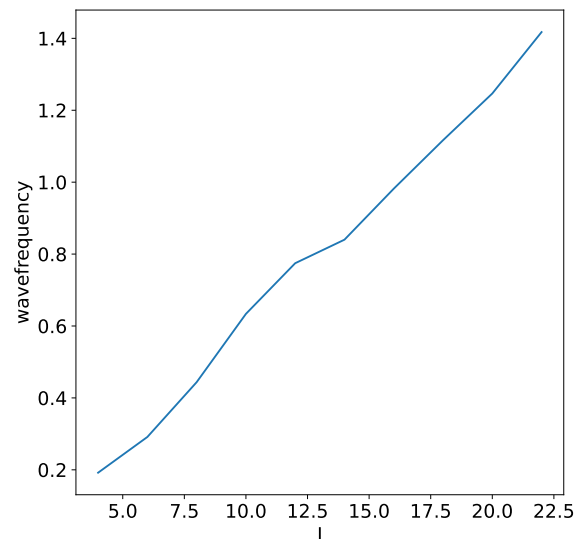


Figure 6: Evolution of the wavefrequency with respect to the descending input parameter I

It can be seen that both the frequency and wavefrequency grow with the descending input parameter I . Furthermore, they seem to follow the same trajectory, the plots look very much alike except for the range of the values which are $[2, 6] Hz$ for the frequency and $[0.2, 1.4] Hz$ for the wavefrequency. Indeed this makes sense, if the frequency increases, the number of waves observed at each second will also increase in the same manner. Furthermore, the relationship $wavefreq = freq * ipls$ shows that these two are linearly dependent.

Looking at the value of the ptcc around the whole range of I is also interesting, we observe the following:

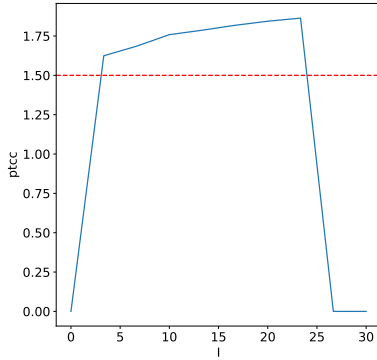


Figure 7: Evolution of the ptcc value with respect to the descending input parameter I vary

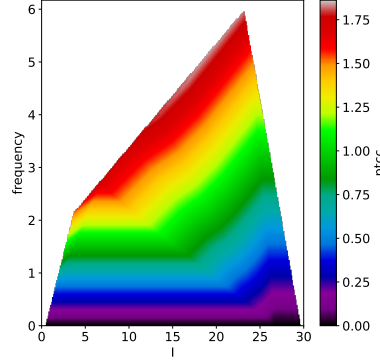


Figure 8: Evolution of the ptcc when the frequency and the descending input parameter I vary

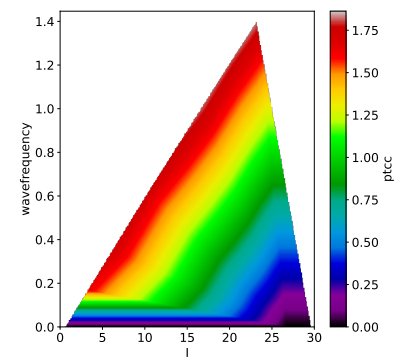


Figure 9: Evolution of the ptcc when the wavefrequency and the descending input parameter I vary

It can be observed that the higher the descending input parameter, the higher the frequency and wavefrequency and the higher the ptcc. This means that the fish is more stable when its frequencies are higher. However, we must remember that there is a limit to this conclusion past which the value of the ptcc metric starts to decrease.

Seeing that the frequency increases when the input drive increases makes sense because this means that the excitatory signal that is sent from the the last CPG neurons to the muscle cells will be stronger and will yield more movement. They will need a fewer number of input signals since they are stronger.

However, if the parameter I increases too much, the inhibitory connections between CPG neurons becomes too consequent such that the last layer of neurons are inhibited for too long and cannot provide reliable excitatory signals to the muscle cells.

5. Test the firing rate controller swimming behavior and turning

In exercises 3 and 4 you have simulated the firing rate controller, but not the neuromechanical zebrafish model. Run an individual simulations with default parameters, visualize the swimming behavior and test its performance. Next, test the ability of the turning by applying a differential drive $I_{diff} \in [0, 4]$ (run a parameter sweep in this interval). To measure the turning performance, you can use the curvature and lateral speed metrics. Check that the turning radius match the curvature expected from the trajectory (i.e. plot the center of mass trajectory and the compute the radius=1/curvature). Plot a swimming trajectory and neuron activities for fixed $I_{diff} = 0$ and $I_{diff} > 0$. How does the activities of left and right CPGs and MCs change for the case $I_{diff} > 0$?

5. Answer

5.1. Swimming behavior of neuromechanical zebrafish, individual simulation

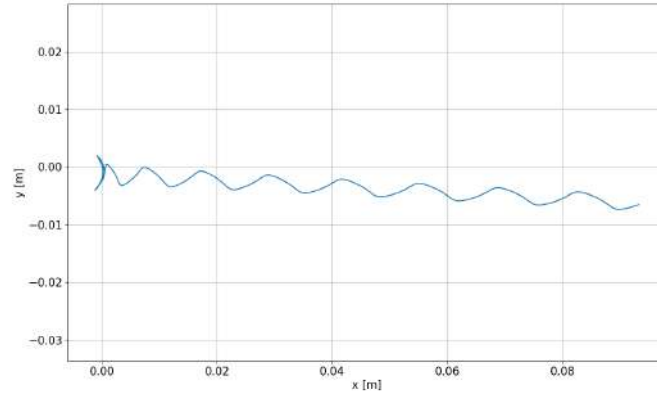


Figure 10: Trajectory of head of zebrafish with default parameters, and 3001 iterations.

The fish is going forward, by oscillating its tail. The computed forward speed cycle is around $0.046 m.s^{-1}$.

5.2. Measuring turning performance

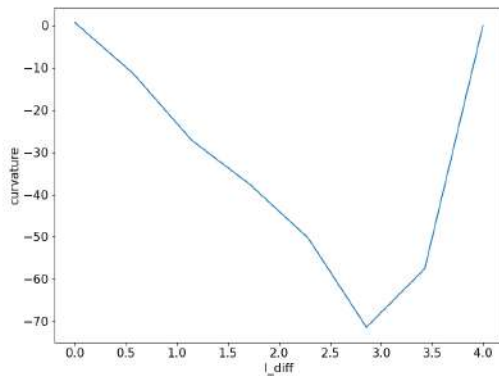


Figure 11: Curvature with respect to differential drive ($nsim=8$).

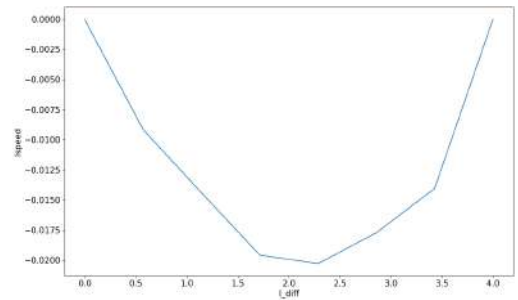


Figure 12: Lateral speed with respect to differential drive ($nsim=8$).

It can be seen in Figures 11 and 12 the effects on the curvature and lateral speed when applying a non zero differential drive. Regarding the curvature, its absolute value is drastically increasing until $L_{diff} = 2.9$. After this stage, the curvature is dropping to reach the initial 0 curvature at $L_{diff} = 4$.

An equivalent behavior is noted regarding the lateral speed: its absolute value increases until a critical $L_{diff} = 2.4$ where the lateral speed is going back to 0.

This can be explained by the firing rate equations of the left and right CPG units: L_{diff} is added in the argument of decision function of the left firing rate equation, while it is removed for the right units. The asymmetry introduced by this differential drive produces more contraction on the left side, leading to a higher torque. This higher activity level pushes more strongly the fish against the water, causing it to curve towards the opposite side.



Figure 13: Left oscillation ($I_{diff}=2$).

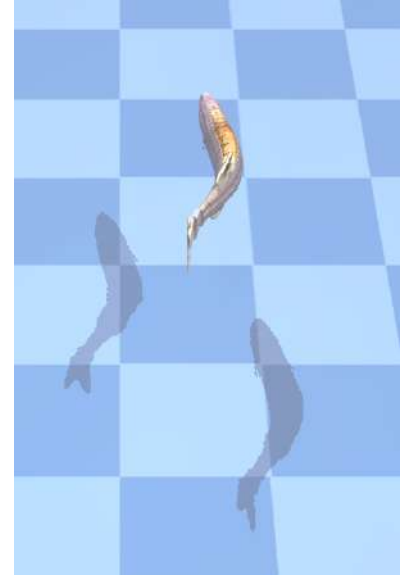


Figure 14: Right oscillation ($I_{diff}=2$).

This asymmetry in motion is well captured in Figures 13 and 14: the maximum torsion when the left units are contracted is more extreme than when the right units are activated. This leads in a turning motion towards the left.

But when I_{diff} becomes too large compared to I , the right units never reach a positive value, which results to 0 spikes due to the decision function: $F = \sqrt{\max(x, 0)}$. There is then no more oscillation since the right units are not activated. For example, at $I_{diff} = 4$ the fish stays in the same disposition as in Figure 13, and its forward and lateral speeds are 0.

The plot 15 shows the center of mass trajectory when applying a nonzero differential drive ($I_{diff} = 1$). A circle is then fitted to this trajectory, and its radius is extracted. The radius of this fitted circle is found to be 0.0359m, while $1/\text{curvature}$ is -0.0418m, which confirms that the turning radius matches the curvature expected.

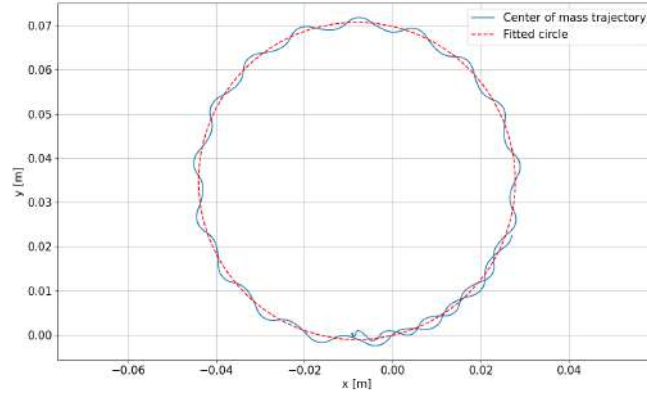


Figure 15: Trajectory of center of mass with $I_{diff}=1$ and 7001 iterations.

5.3. CPGs and MCs activities depending on I_{diff}

Figure 22 shows the differences in activation units depending on the value of I_{diff} .

When $I_{diff} = 0$ (figures 16 and 17), there is a symmetry in activation between left and right units: when left CPG units are activated, the right ones are not, and the activation time seems balanced between the two sides. This is also reflected in the muscles unit where symmetrical contractions are observed.

When $I_{diff} = 2$ (figures 18 and 19), there is a clear asymmetry between both sides: the left CPG units are activated longer than the right units. This impacts the muscles units which show broader spikes for the left side, compared to thinner peaks for the right units. This explains well the turning behaviour observed just before: when there is no differential drive, the muscles are active for a same time duration. But when an asymmetric descending input is introduced, the left muscles unit contract for a longer period, which results in a turning motion.

But when $I_{diff} = 4$ (figures 20 and 21), the differential is too large between both sides: the right side remains inactive because of a negative argument in the argument of the gain function F . The left CPG units on the contrary remains active, since there is no counter activation on the right side. This explains the left torsion equivalent to Figure 13 which remains at all time step when the differential drive is too large.

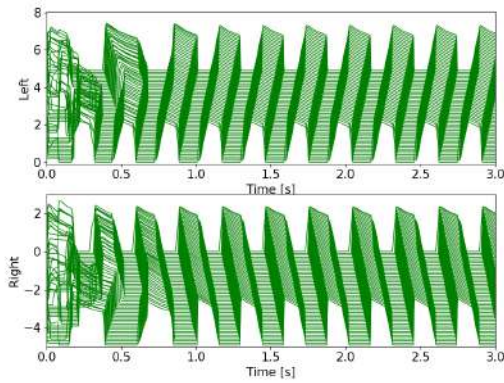


Figure 16: CPG activation for $Idiff=0$

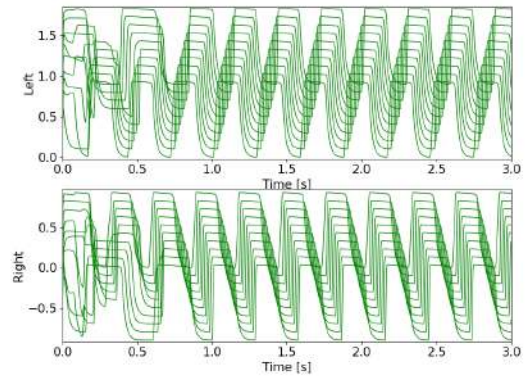


Figure 17: Muscle activation for $Idiff=0$

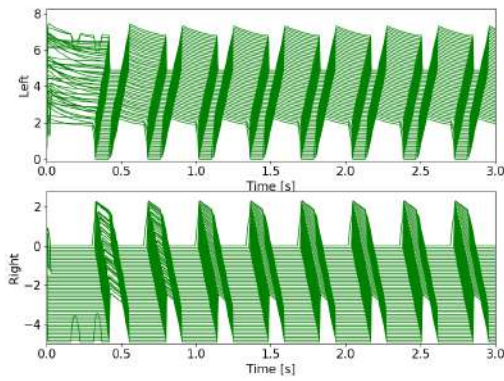


Figure 18: CPG activation for $Idiff=2$

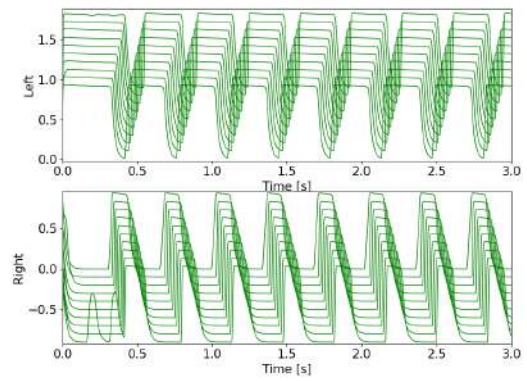


Figure 19: Muscle activation for $Idiff=2$

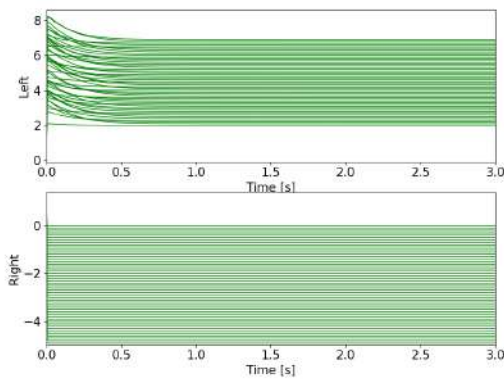


Figure 20: CPG activation for $Idiff=4$

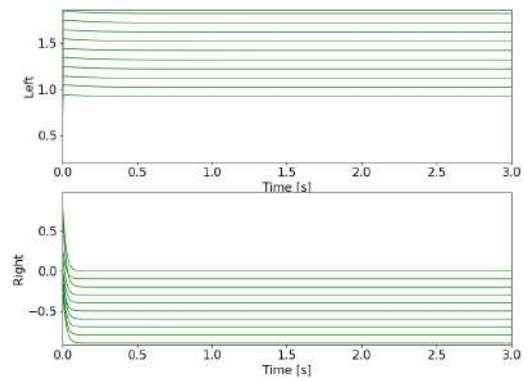


Figure 21: Muscle activation for $Idiff=4$

Figure 22: Differences in activation depending on the differential drive input.

6. Implement the feedback equations and test different feedback weights

Implement now the feedback equations and add stretch feedback to the CPG oscillators ($g_{ss} > 0$), i.e. implement the full network ?? and test the role of the stretch feedback to the controller for fixed parameters. Plot the activities of CPG neurons, muscle cells and sensory neurons and that of the joint angle positions. Now vary $g_{ss} \in [0, 15]$, how does the frequency, wavefrequency and forward speed change? Is feedback beneficial for a good swimming performance? Under which conditions?

6. Answer

6.1. Role of sensory feedback for fixed parameters

The increased feedback weight g_{ss} enhances the influence of the sensory feedback on the CPG neurons (Figure 26). This stronger coupling increases the sensitivity of the CPG neurons to the sensory feedback, leading to an increased firing rate. The heightened firing rate of the CPG neurons then causes more frequent muscle activation (Figure 30), and the sensory feedback units also become more active (Figure 34), perpetuating the cycle. This results in an overall increase in the frequency of firing rates for the CPG neurons, muscle units, and sensory feedback. Consequently, a higher frequency of muscle contractions results in more rapid oscillations of the joint angles (Figure 38). This means the joints will move back and forth more frequently, reflecting the increased dynamic activity in the underlying neuromuscular system.

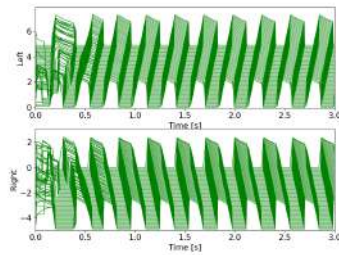


Figure 23: $g_{ss}=0$

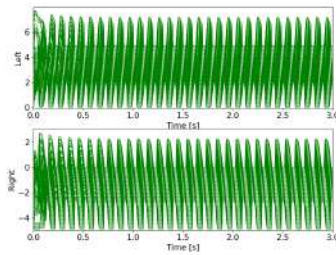


Figure 24: $g_{ss}=5$

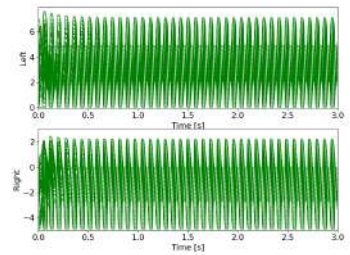


Figure 25: $g_{ss}=10$

Figure 26: CPG activation for different feedback weights.

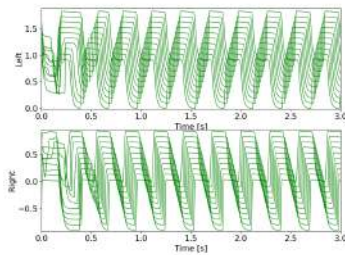


Figure 27: $g_{ss}=0$

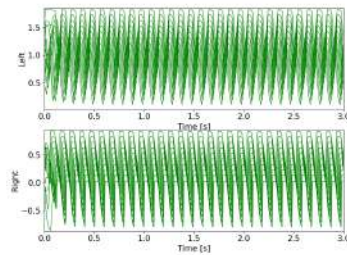


Figure 28: $g_{ss}=5$

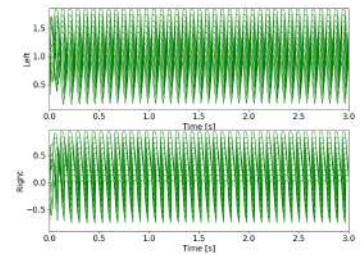


Figure 29: $g_{ss}=10$

Figure 30: Muscle activation for different feedback weights.

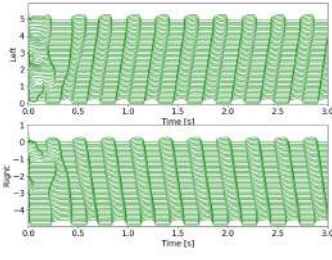


Figure 31: $g_{ss}=0$

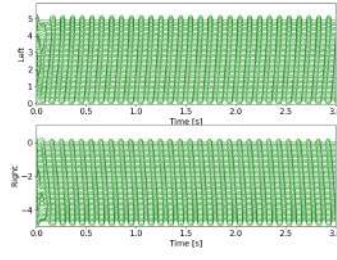


Figure 32: $g_{ss}=5$

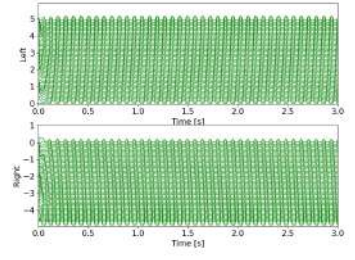


Figure 33: $g_{ss}=10$

Figure 34: SS activation for different feedback weights.

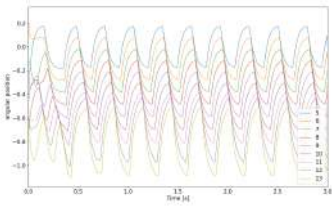


Figure 35: $g_{ss}=0$

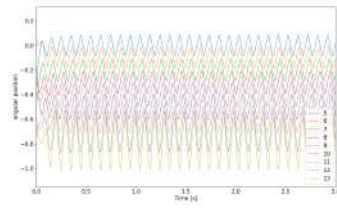


Figure 36: $g_{ss}=5$

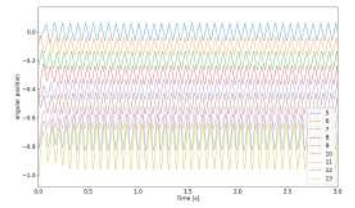


Figure 37: $g_{ss}=10$

Figure 38: Joints activation for different feedback weights.

6.2. Influence of the feedback weight on the frequency, wave frequency and forward speed

As seen in Figure 39, an increase in feedback weight g_{ss} increases the frequency. Indeed, the frequency refers here as the number of oscillations or firing events per unit time. It indicates how rapidly the neurons and muscles are cycling through their activity phases. As observed previously, an increase in g_{ss} enhances the firing rate of individual CPG neurons and muscle units because they respond more robustly to the increased feedback.

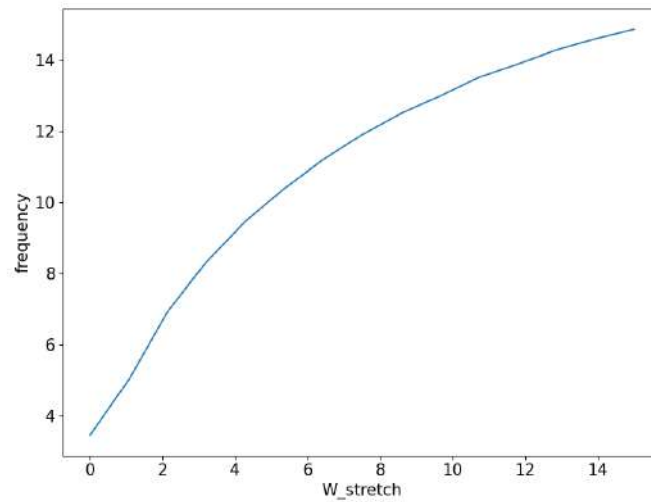


Figure 39: Frequency with respect to g_{ss} , for $g_{ss}=[0,15]$, $nsim=15$ and $niterations=10001$

It can be noted on Figure 40 that the wave frequency increases with g_{ss} , but up to a certain point (around $g_{ss} = 4$), from which the wave frequency drops, and reaches a lower stage. The wave frequency refers here as the frequency of the overall locomotor pattern generated by the system. It reflects the frequency of the whole-body undulations produced by the sequential activation of muscles along the body. It is then dependent on the precise coordination and timing of the oscillatory activity of multiple CPG neurons and muscles. Indeed, beyond $g_{ss} = 4$, the over-strengthened feedback disrupts the coordination among CPG neurons and muscles. As a result, the effective wave frequency decreases even though individual firing rates continue to increase.

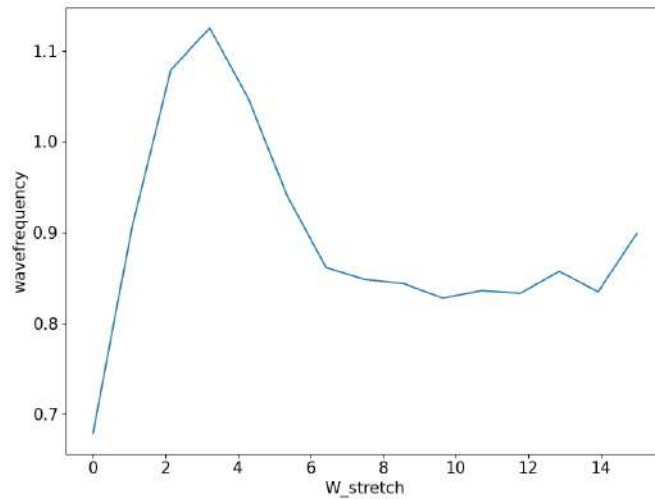


Figure 40: Wave frequency with respect to g_{ss} , for $g_{ss}=[0,15]$, $nsim=15$ and $niterations=10001$

The Figure 41 shows interesting results regarding forward speed performance depending on g_{ss} : the speed approximately increases until $g_{ss} \approx 8$, and then slowly decreases for all $g_{ss} > 8$. This means that when g_{ss} is too high, it can lead to over-excitation of neurons, causing them to fire too frequently. This rapid firing can prevent the proper buildup of the motor commands required for effective muscle contractions. It can indeed be noted that when g_{ss} increases, the fish undulates less. It is an efficient swimming up to a certain point, after which the tail doesn't propel the body enough to maintain high speeds.

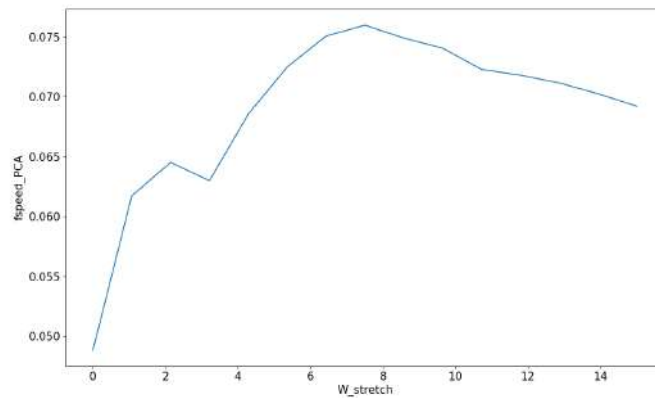


Figure 41: Forward speed PCA with respect to g_{ss} , for $g_{ss}=[0,15]$, $nsim=15$ and $niterations=10001$

6.3. Conditions under which feedback weight is beneficial

Combining sensory feedback and CPG units seems to be beneficial for the performance of the fish: feedback from stretch sensors could compensate not well tuned CPG units, by giving direct information on the state of the model. But giving too much weight to the sensory feedback can be counterproductive: over-strengthened feedback could disrupt the coordination among CPG neurons and muscles, leading to inefficient swimming with not enough oscillations due to over-excitation.



Figure 42: $g_{ss}=0$, $f_{speed} = 0.0448$

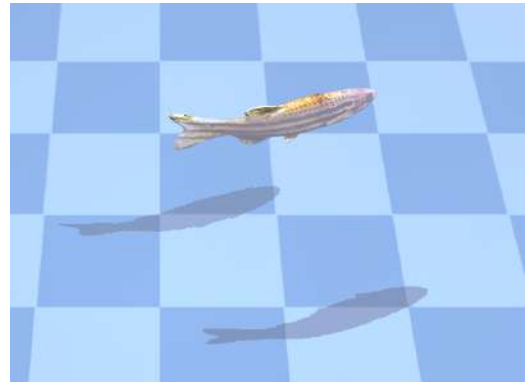


Figure 43: $g_{ss}=7$, $f_{speed} = 0.0610$

Figure 44: Maximum amplitudes of the tail when varying the feedback weight

As seen in Figure 44, when increasing g_{ss} , only the last joints undulate, due to higher attention on stretch sensors, resulting in smaller amplitudes of oscillations. It was found that maximum forward speeds are achieved around $g_{ss} \approx 7$, after which the speed decreases, since the oscillations become too small.

7. Explore the dependency on the descending input I and feedback weight g_{ss}

Repeat the analysis of question 5 for different values of $g_{ss} \in [0, 15]$. How does the frequency and wave-frequency change with the added feedback? Does the ranges of inputs I leading to stable oscillation change? What about the performance (i.e. forward speed) for these ranges of I , does it change?

7. Answer

7.1. Repeat analysis of question 5 for different values of g_{ss}

We try with a few different values of g_{ss} . The values chosen were: [5,10,15].

Measuring turning performance:

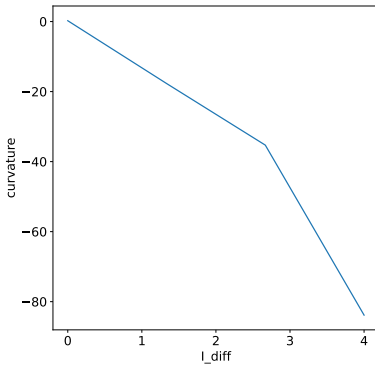


Figure 45: Curvature for $g_{ss} = 5$

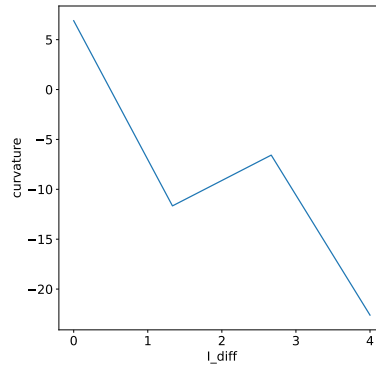


Figure 46: Curvature for $g_{ss} = 10$

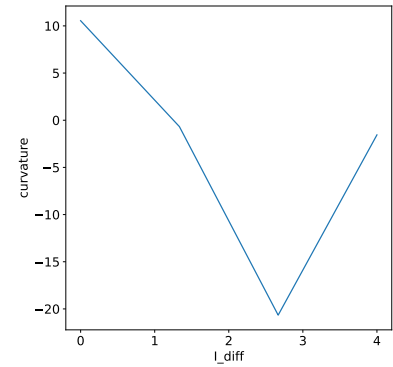


Figure 47: Curvature for $g_{ss} = 15$

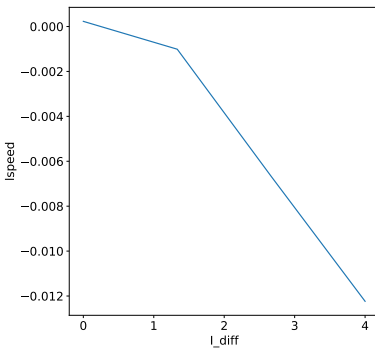


Figure 48: Speed for $g_{ss} = 5$

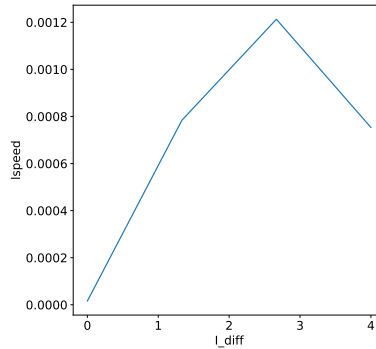


Figure 49: Speed for $g_{ss} = 10$

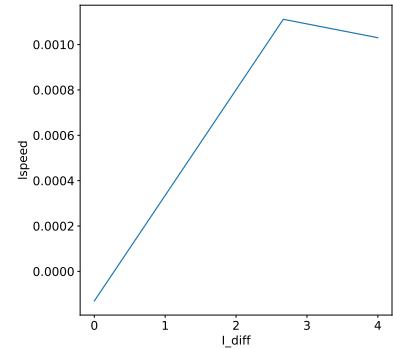


Figure 50: Speed for $g_{ss} = 15$

It can be seen in Figure 45, 46 and 47 the effects on the curvature and lateral speed when applying a non zero differential drive, with a added feedback.

We can look at the effects of feedback on curvature and lateral speed using different values of g_{ss} . For $g_{ss} = 5$, the curvature decreases sharply from approximately 0 to -80 as L_{diff} increases from 0 to 4, indicating a strong inward curve. With $g_{ss} = 10$, the curvature starts at around 5, fluctuates, and decreases to -20, showing a less pronounced but more variable inward curve. For $g_{ss} = 15$, the curvature begins at 10, dips to -20, and slightly recovers, suggesting a complex curvature pattern.

The feedback's impact on lateral speed is seen in Figures 48, 49, and 50. For $g_{ss} = 5$, the speed steadily decreases from 0 to -0.012 as L_{diff} increases. When $g_{ss} = 10$, the speed exhibits a dynamic response, peaking at 0.0012 before declining. Similarly, for $g_{ss} = 15$, the speed rises to a peak of 0.0010 and then goes down. These observations indicate that higher values of g_{ss} lead to less sharply

negative but more variable curvature and dynamic speed responses, reflecting the system's sensitivity to feedback adjustments.

In conclusion, feedback significantly influences the curvature of the system, with varying effects depending on the value of g_{ss} . This highlights the critical role of feedback in controlling and modulating the curvature of the system, showing the need to carefully adjust feedback parameters to achieve desired curving behaviors. Higher feedback tends to better curvature movement.

7.2. How does the frequency and wavefrequency change with the added feedback? Does the ranges of inputs I leading to stable oscillation change? What about the performance (i.e. forward speed) for these ranges of I , does it change?

For each values, we will plot how the frequency and wave frequency change with the added feedback. To measure the performance we will also plot the fspeed and the ptcc. To verify wether or not the range of input I leads to stable oscillations, we start with the values from $[0;30]$ then vary it afterwards, for every value of g_{ss} .

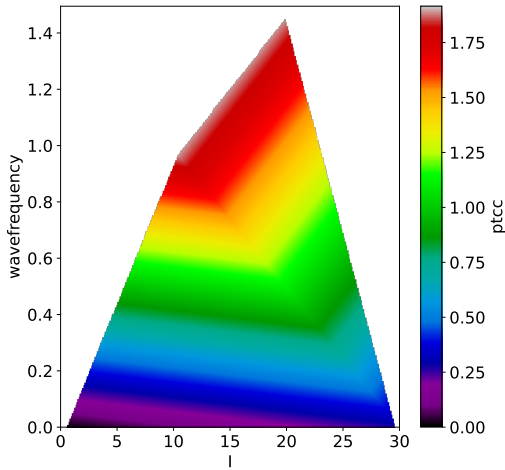


Figure 51: Evolution of the ptcc with wavefrequency and I for $g_{ss} = 5$

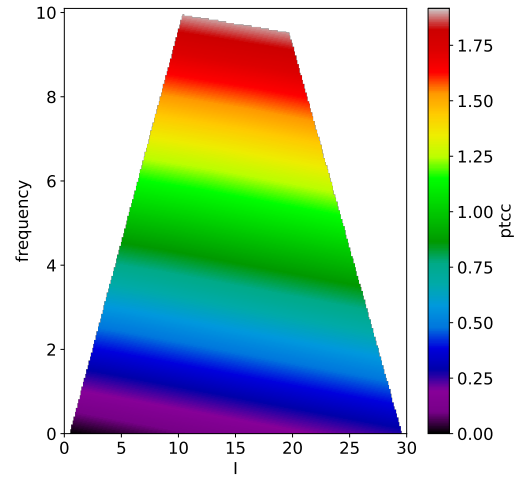


Figure 52: Evolution of the ptcc with frequency and I for $g_{ss} = 5$

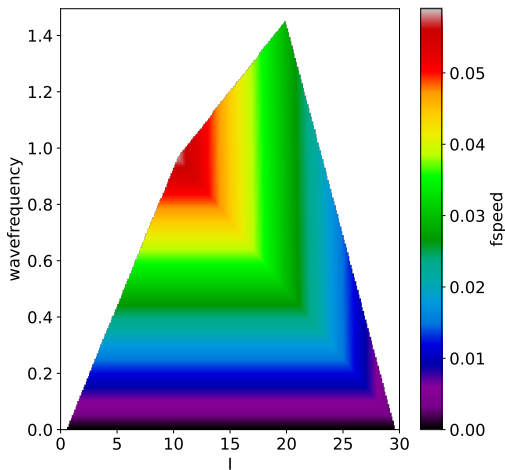


Figure 53: Evolution of the fspeed with wavefrequency and I for $g_{ss} = 5$

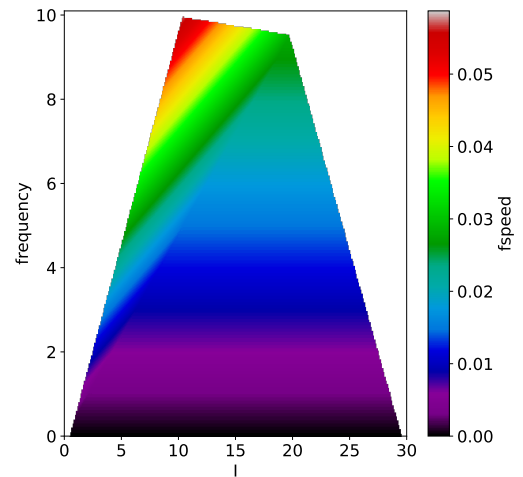


Figure 54: Evolution of the fspeed with frequency and I for $g_{ss} = 5$

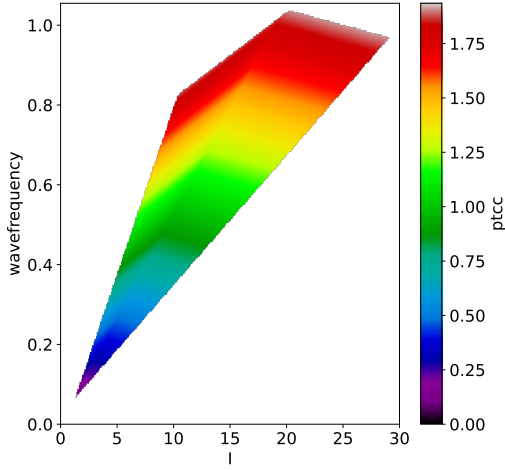


Figure 55: Evolution of the $ptcc$ with wavefrequency and I for $gss = 10$

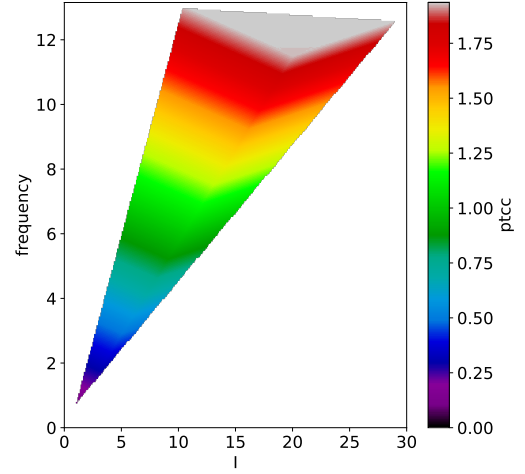


Figure 56: Evolution of the $ptcc$ with frequency and I for $gss = 10$

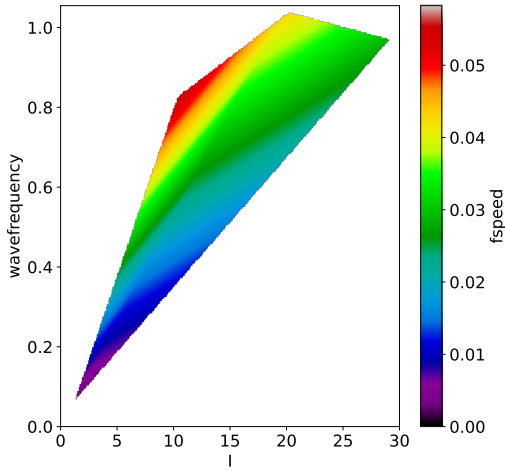


Figure 57: Evolution of the $fspeed$ with wavefrequency and I for $gss = 10$

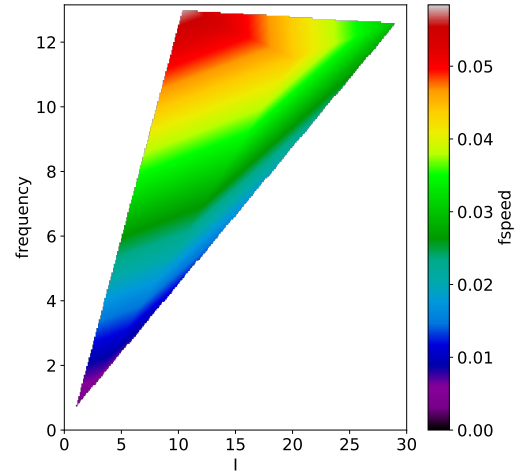


Figure 58: Evolution of the $fspeed$ with frequency and I for $gss = 10$

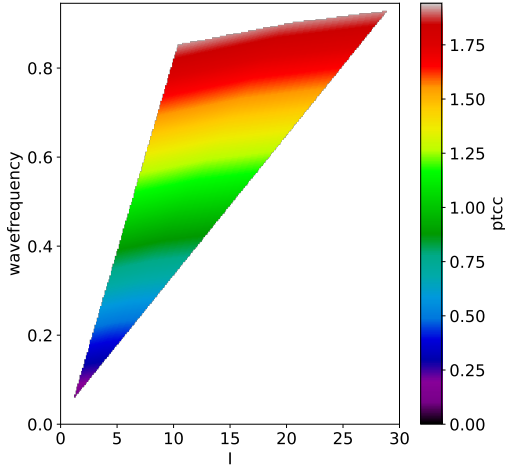


Figure 59: Evolution of the ptcc with wavefrequency and I for $g_{ss} = 15$

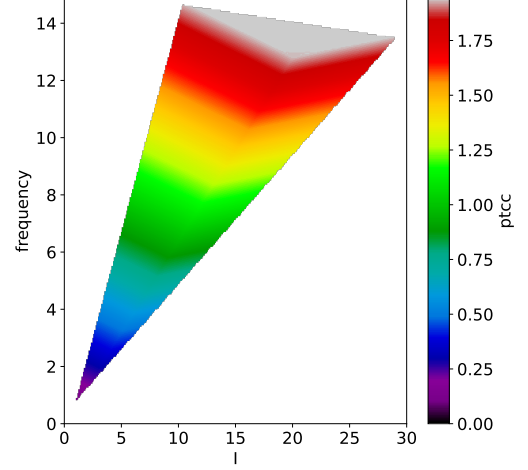


Figure 60: Evolution of the ptcc with frequency and I for $g_{ss} = 15$

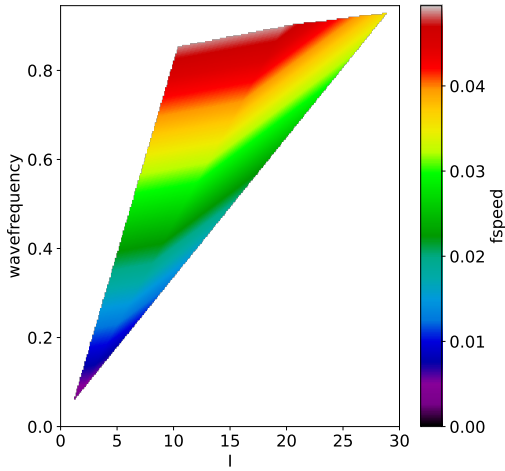


Figure 61: Evolution of the fspeed with wavefrequency and I for $g_{ss} = 15$

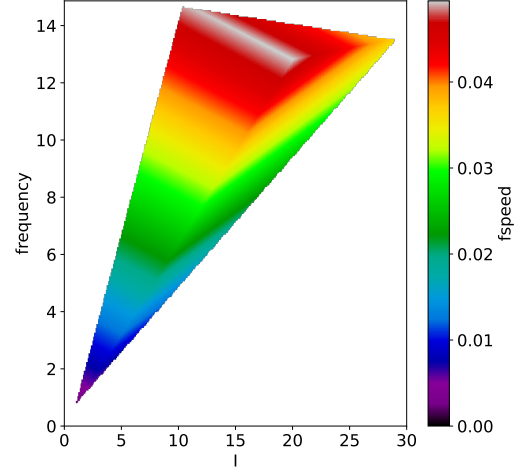


Figure 62: Evolution of the fspeed with frequency and I for $g_{ss} = 15$

Based on the provided figures, we can draw several conclusions regarding the effects of added feedback on frequency, wavefrequency, input ranges leading to stable oscillation, and performance (forward speed).

The figures show the evolution of ptcc and fspeed as the wavefrequency and frequency vary with different values of g_{ss} . As g_{ss} increases from 5 to 15, the range of frequencies and wavefrequencies where stable oscillations occur shifts and increases. For lower values of g_{ss} , the changes in ptcc and fspeed are more gradual, but as g_{ss} increases, the variations become more pronounced, showing steeper gradients. This suggests that higher feedback values amplify the changes in frequency and wavefrequency, resulting in more significant adjustments to the oscillatory behavior of the system.

The input parameter I is critical for maintaining stable oscillations. The figures indicate that as g_{ss} increases, the range of I values leading to stable oscillations expands. For $g_{ss} = 5$, stable oscillations occur within a narrower range of I values, as seen in the more confined regions of ptcc and fspeed. In contrast, for $g_{ss} = 10$ and $g_{ss} = 15$, the stable regions become broader, allowing for a wider range of I values to achieve stable oscillations. This broader range suggests that increased feedback improves the system's tolerance to variations in I , enhancing stability over a larger parameter space.

The performance, measured as forward speed (fspeed), also varies with the changes in I and g_{ss} .

For $g_{ss} = 5$, the forward speed shows relatively modest increases within the stable range of I . As g_{ss} increases to 10 and 15, the forward speed not only increases but also displays more pronounced peaks within the stable oscillation ranges. This indicates that higher feedback values not only broaden the stable range of I but also enhance performance by enabling higher forward speeds. The figures demonstrate that with higher g_{ss} , the system can achieve better performance, reflected in the increased forward speeds for a wider range of input parameters.

These observations highlight the importance of feedback in optimizing both stability and performance of the system, providing valuable insights for tuning the feedback parameters to achieve desired operational characteristics.

8. Explore the effect of noise with/o feedback

Let us now consider the effect of noise in the system and test the robustness of the network to noise. You will add noise to the activity variables of the CPG neurons in equation ???. We consider two vector of Ornstein-Uhlenbeck processes $\underline{x}_t = (x_{t_0}, \dots, x_{t_{49}})$ (for the left neurons) and $\underline{y}_t = (y_{t_0}, \dots, y_{t_{49}})$ (for the right neurons):

$$\begin{aligned} dx_t &= -\theta \underline{x}_t \cdot dt + \sigma dW_t \\ dy_t &= -\theta \underline{y}_t \cdot dt + \sigma dW_t \end{aligned} \quad (1)$$

Where $\theta > 0$ and $\sigma > 0$ are parameters, and W_t is a Weiner process. Here, we choose $\theta = 0.1$. The CPG activity equations in ??? will now be modified by adding the noise terms according to:

Implement in `firing_rate_controller.py::get_ou_noise_process_dw` an Euler-Maruyama scheme for solving numerically the Ornstein-Uhlenbeck process.

Internally (you do not need to implement this!), the solution of the Euler-Maruyama scheme will be added to the original system's variables to solve the CPG activities with added noise:

$$\begin{aligned} \tau \dot{r}_L &= -r_L + F(I - ba_L - g_{in} W_{in} \cdot r_R - g_{ss} W_{ss} \cdot s_R) + \underline{x}_t \\ \tau \dot{r}_R &= -r_R + F(I - ba_R - g_{in} W_{in} \cdot r_L - g_{ss} W_{ss} \cdot s_L) + \underline{y}_t \end{aligned} \quad (2)$$

Now that you have added the noise process in the system, run a two parameter search, varying $\sigma \in [0, 30]$ and $w_{stretch} \in [0, 10]$. Is the feedback helpful to stabilizing the oscillations and performance under noise (use the speed PCA metric to evaluate the performance, as it is less sensitive to the noise)?

Note: when adding noise in the system, you should not consider the frequency and wavefrequency metrics, as they could be corrupted by the noise.

8. Answer

We complete the function `firing_rate_controller.py::get_ou_noise_process_dw` following this :

```
def get_ou_noise_process_dw(self, timestep, x_prev, sigma):
    """
    Implement the integration of the Ornstein-Uhlenbeck processes using the Euler-Maruyama method.
    dx_t = -0.5*x_t*dt + sigma*dW_t
    Parameters
    -----
    timestep: float
    Timestep size.
    x_prev: np.array
    Previous state of the OU process.
    sigma: float
    Noise level, standard deviation of the Wiener process increment.
    Returns
    -----
    np.array
    Next state of the OU process.
    """
    # Generate Wiener increments
    dW = np.random.normal(loc=0.0, scale=np.sqrt(timestep), size=x_prev.shape)

    # Calculate the increment in the Ornstein-Uhlenbeck process
    dx_process = -0.1 * x_prev * timestep + sigma * np.sqrt(timestep) * dW

    # Update the process value
    x_new = dx_process
```

```
return x_new
```

Now that the code is complete, we run a two parameter search, varying $\sigma \in [0, 30]$ and $w_{stretch} \in [0, 10]$.

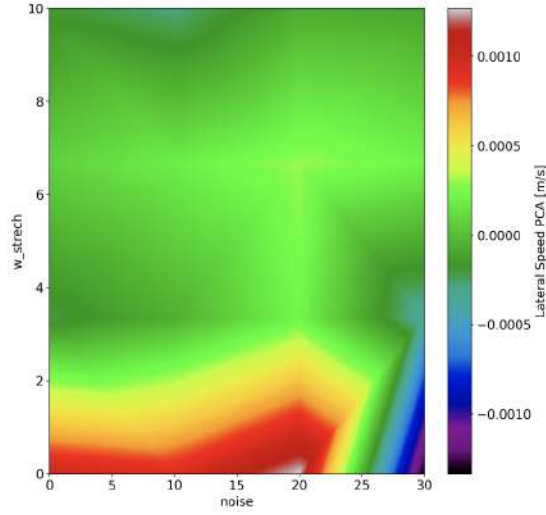


Figure 63: Parameter search for w and σ , using the PCA metric

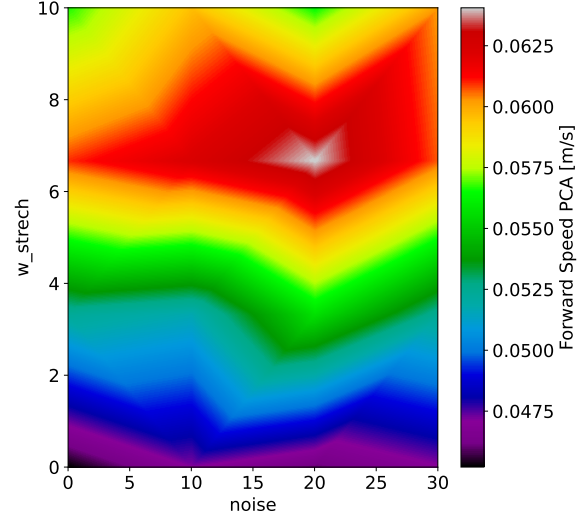


Figure 64: Parameter search for w and σ , using the PCA metric

We push the noise and $w_{stretch}$ to more specific values to figure out what the range is for the best values for lateral and forward speed.

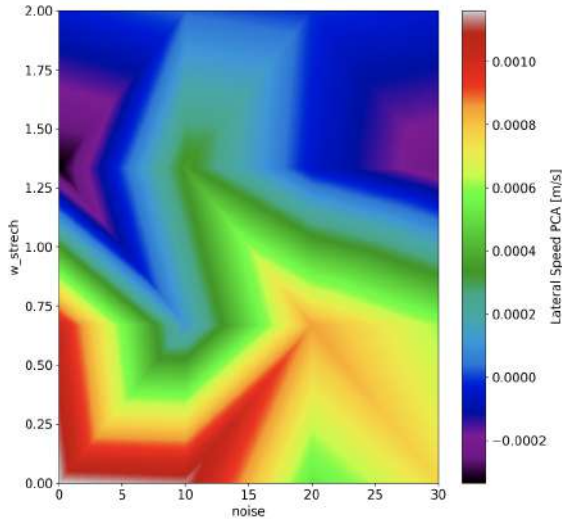


Figure 65: Parameter search for w and σ , using the PCA metric

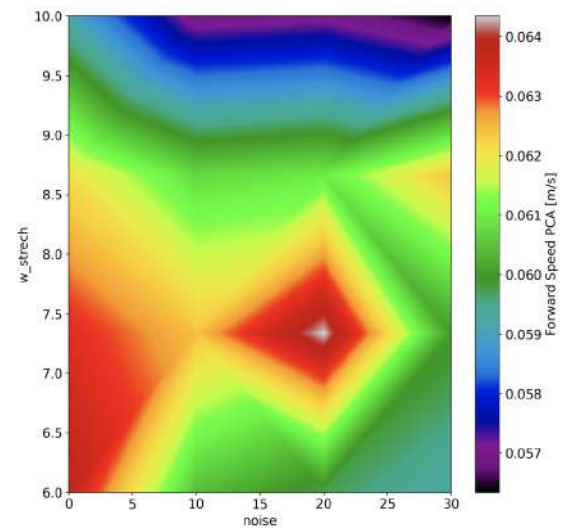


Figure 66: Parameter search for w and σ , using the PCA metric

Lets talk about the lateral speed :

1. Fig. 63 shows the parameter search for w and σ (noise) using the PCA metric for lateral speed. The lateral speed PCA values range from approximately -0.0010 to 0.0010. The effect of

$w_stretch$ is clear here. It shows that with it, it reduces the lateral speed, getting to zero and the fish can now swim better.

2. Fig.65 Further refines the search for w and σ , showing similar patterns.

Forward Speed PCA:

1. Fig. 64 illustrates the parameter search for w and σ using the PCA metric for forward speed. The forward speed PCA values range from approximately 0.0475 to 0.0625. It shows that even with noise, higher values of $w_stretch$ leads to better forward speed.
2. Fig. 66 provides a more specific search range for w and σ .

The feedback appears to help in stabilizing the lateral oscillations as indicated by the lateral speed PCA values remaining close to zero with higher values of feedback. The lateral speed performance is more sensitive to noise, and the feedback helps in maintaining stability.

The forward speed PCA metric shows that performance improves with higher w stretch and moderate levels of noise (σ). This suggests that feedback enhances performance by enabling the system to maintain higher forward speeds even in the presence of noise. The feedback is beneficial in achieving higher forward speeds while maintaining stability, as evidenced by the PCA metric.

9. Open question

Open questions. These questions are meant to assess your understanding of the topics addressed during the project. You should reply in a concise, scientific way by explaining your reasoning and listing the reference literature to support your idea.

1. During the project, you tested the effect of proprioceptive sensory feedback with varying levels of noise. How would you design a biological experiment to validate in-vivo the simulation results?
2. What other aspects of zebrafish locomotion could be affected by the presence (or absence) of proprioceptive sensory feedback? How would you test those hypotheses in simulation and biological experiments?
3. What other types of sensory feedback could play a role during zebrafish locomotion? How would you disambiguate the relative contribution of the different sensory feedback modalities? How can simulation help in addressing this problem?

9. Answer

1. To validate the simulation results on the effect of proprioceptive sensory feedback with varying levels of noise, we can do an in-vivo experiment using zebrafish. For this, we would need to find a way to introduce noise to the activity variables of the CPG neurons in the zebrafish. One way of doing this could be with optogenetic methods which would disturb neuronal activity when a light is presented and simulate the noise we have added in the system.

When the light is turned on and the optogenetic stimulation disturbs the CPGs, the motor outputs of the muscle activations can be recorded and analysed in order to then validate the simulation results. This experiment would then be done on two groups of zebrafish samples: a control group, with normal proprioceptive feedback, and an experimental group, for which stretch sensor neurons would have been disabled (via pharmacological, genetical, or mechanical manipulation). This way it could be interesting to see if the control group perform motion better. This could then validate the role of sensory feedback as a "tuner" for CPG's units.

2. The presence or absence of proprioceptive sensory feedback can significantly impact zebrafish locomotion in terms of swimming efficiency, coordination, and adaptability to environmental changes. To test these hypotheses, we can do both simulation and biological experiments. In simulations, we will model zebrafish swimming with varying levels of proprioceptive feedback to measure swimming speed, energy consumption, intersegmental coordination, and adaptability to virtual environmental perturbations. These combined approaches will provide a comprehensive understanding of the role of proprioceptive feedback in zebrafish locomotion.

In biological experiments, these can be tested through optogenetic stimulation as mentioned in the previous question. For example, the coordination of the zebrafish impacted by sensory feedback can be tested if we remove this feedback and observe the resulting swimming of the fish. Another way of doing this could be through varying environments such as calm waters, water currents, and very unstable water environments. These could result in different swimming patterns in the zebrafish and yield to a conclusion.

3. There are different types of sensory feedback. They include: (See CMC lecture [?])

- **Spinal**

- **Muscle spindles:** provide information about **length**, and **velocities** (changes of lengths) of muscles
- **Golgi tendon organs:** provide information about (internal) **force** (i.e., tension) in muscle
- **Cutaneous receptors:** provide information about **contact forces**

- **Stretch sensitive cells** in the spinal cord itself (as found in lamprey and zebrafish)
- **Supraspinal**
 - **Vestibular system**: provides the sense of **balance**, rotational and linear **accelerations**
 - **Visual system**: very rich information about visual scene, **optical flow**, colors, edges, patterns, etc.

In zebrafish, certain spinal sensory modalities such as **stretch sensitive cells** and **cutaneous receptors** play crucial roles. Stretch sensitive cells in the spinal cord provide vital feedback for maintaining posture and locomotion. Cutaneous receptors in zebrafish offer information about contact forces, aiding in the detection of environmental interactions. To disambiguate the relative contribution of different sensory feedback modalities, we can use computational simulations. Computational simulations can model the integrated sensory feedback mechanisms to predict outcomes under various conditions, allowing to study the complex interactions between different sensory inputs. This is what has been done in this project, removing and adding those sensory feedbacks to assess their performances.

In order to make sure that we are looking at only one sensory feedback at a time, we need to disambiguate the relative contribution of the different sensory feedback modalities. This can be done by physically removing these sensory inputs from the zebrafish (example : covering its eyes to remove visual sensory input) or designing experiments which we know will only impact one sensory modality. For this to work, the different behaviours can be compared when one or multiple sensory feedback modalities are active. This would allow the user to see the variations when a sensory modality is present or not.

References

1. EPFL Moodle. *Lecture 8: Reflexes and Sensory Feedback*. Retrieved from https://moodle.epfl.ch/pluginfile.php/1598258/mod_resource/content/11/lecture8_Reflexes_Sensory_Feedback.pdf